ELSEVIER

Physica C 301 (1998) 315–325

PHYSICA C

Site occupancy and T_c degradation in iron substituted $YBa_2(Cu_{1-x}Fe_x)_4O_{8+\delta}$

T. Akachi [a,*], R. Escamilla [a], V. Marquina [b], M. Jiménez [b], M.L. Marquina [b], R. Gómez [b], R. Ridaura [b], S. Aburto [b]

[a] *Instituto de Investigaciones en Materiales, UNAM, 04510 México D.F., Mexico*
[b] *Facultad de Ciencias, UNAM, 04510 México D.F., Mexico*

Received 22 July 1997; revised 3 March 1998; accepted 9 April 1998

Abstract

A series of $YBa_2(Cu_{1-x}Fe_x)_4O_{8+\delta}$ samples with $x = 0.00625$, 0.0125, 0.01875, 0.025 and 0.05, were synthesized and characterized by resistance vs. temperature measurements, X-ray diffraction and by Mössbauer spectroscopy. In order to make the site assignment for the Fe atoms, a Rietveld refinement of the X-ray spectra was performed and a point charge calculation of the quadrupole splitting for all the possible oxygen environments around the two Cu sites was carried out, taking into account the two possible ionic states of the iron atoms that occupy those sites. We found that, for low level iron concentrations, the Fe atoms occupy only the Cu(1) sites of the structure in a fivefold pyramidal coordination, with the apical oxygen atom placed along the *a*-axis between the double chains of the unit cell. The presence of these extra oxygen atoms in the crystal structure could be related to the rapid T_c reduction as iron concentration increases.

PACS: 74.25; 74.10; 74.62; 76.80

Keywords: High T_c superconductors; Y1:2:4 system; Iron substitution; T_c degradation; Mössbauer spectroscopy; Rietveld refinement; Site occupancy

1. Introduction

Since the discovery of the $YBa_2Cu_4O_8$ superconducting phase (1:2:4) as a lattice defect in $YBa_2Cu_3O_{7-\delta}$ (1:2:3) [1,2], extensive studies have been done in order to accomplish bulk synthesis at high oxygen pressures [3,4] and also at ambient pressure [5]. It is now well known that the 1:2:4 crystal structure is closely related to that of the 1:2:3, with a double Cu–O chain (ribbon), instead of a single one, along the *b*-axis of the unit cell. The positions of the Cu atoms in adjacent Cu–O chains differ by $b/2$ along the *b*-axis [1]; this fact leads to a longer *c* parameter of 2.725 nm and to a reduced orthorhombicity of 0.8% [6]. These crystal structures allow for two different Cu sites: Cu(1) with fourfold planar coordination along the chains, or ribbons, and Cu(2) in the CuO_2 planes with a fivefold pyramidal coordination. There are, however, two important differences between both systems: in the first place, the

* Corresponding author.

0921-4534/98/$19.00
PII S0921-4534(98)00176-2

superconducting transition temperature, T_c, of 1:2:4 is lower (80 K) than the one in 1:2:3 (90 K); secondly, in contrast to the high oxygen mobility in 1:2:3, the oxygen content in 1:2:4 is stable (up to 850°C) due to the fact that the oxygen atoms in the double chain are bonded to three Cu atoms instead of two, as in the 1:2:3 structure. As a consequence, both the well known second order orthorhombic to tetragonal phase transition [7] and the superconducting to antiferromagnetic transition observed in 1:2:3 as the oxygen content is lowered, are absent in 1:2:4.

Just as in other high-T_c superconductors, in the 1:2:3 and 1:2:4 phases the substitution of Cu atoms by other transition metal atoms, such as Fe, Zn, Ni and Co, produces a T_c degradation [8,9]. The precise mechanisms of why this phenomenon occurs are still not well understood, and several proposals have been made. These range from purely electronic mechanisms [10] that involve a modification in the charge transfer from chains to planes, to magnetic pair breaking when Cu atoms are substituted by magnetic 3d metal atoms [11].

In particular, when a fraction of the Cu atoms is substituted by Fe atoms, Mössbauer spectroscopy becomes an important tool in the study of the local electric and magnetic environment of the Cu sites where the Fe atoms are expected to reside. Additionally, this technique is capable of giving information of their charge and spin states.

In relation to the Mössbauer parameters (MP) of the observed features in the spectra of the $YBa_2(Cu_{1-x}Fe_x)_4O_{8+\delta}$ system, several researchers [12–14] do not agree either as to their values or to the site assignments made. The aim of this work is to try to clarify the sites occupied by the iron atoms in the 1:2:4 system and how they affect its structure and transport properties. We present resistance vs. temperature measurements, X-ray diffractograms and Mössbauer spectroscopy results for $YBa_2(Cu_{1-x}Fe_x)_4O_{8+\delta}$ samples with different iron concentra-

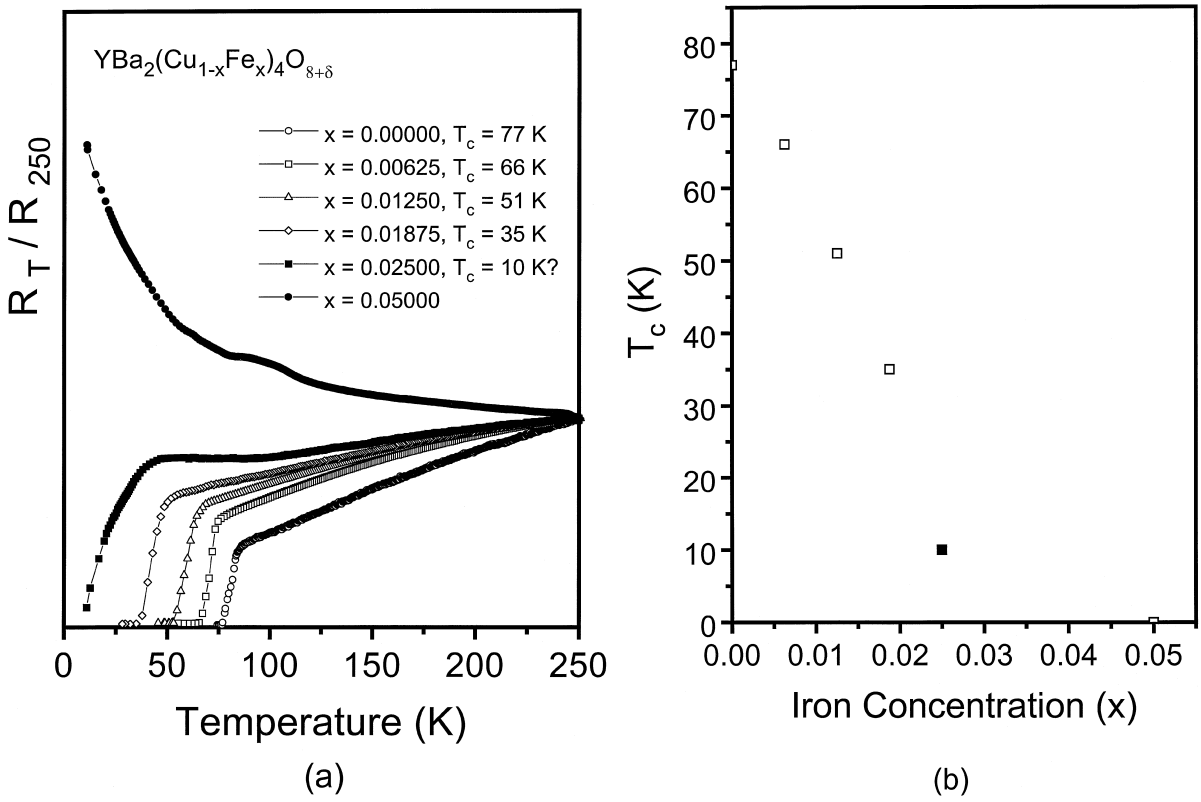

Fig. 1. (a) Normalized resistance vs. temperature of $YBa_2(Cu_{1-x}Fe_x)_4O_{8+\delta}$ samples and (b) T_c variation with iron concentration x.

tions ($x = 0.00625$, 0.0125, 0.01875, 0.025 and 0.05). A Rietveld analysis [15] of the structure was performed, as well as a point charge calculation for all the possible oxygen environments around the two Cu sites, taking into account the two possible ionic states of the iron atoms that occupy those sites. Having this information, a site assignment for the Fe atoms is proposed.

2. Experimental

To synthesize our samples we used a combined method that consists of the following steps: (a) powders of 99.999% pure initial reactants Y_2O_3, $BaCO_3$, CuO and $^{57}Fe_2O_3$ were mixed in stoichiometric quantities, diluted in 10 ml of 96% nitric acid and heated until all the liquid evaporated; the resulting green paste was fired at 700°C in air to obtain small grain (1–10 μm) precursors. (b) The calcinated powders were mixed with sodium nitrate (20% in weight) as catalyst to accelerate the reaction, pressed into pellets, heat treated at 800°C during 20 h in flowing oxygen and slowly cooled (0.5°C/min) to room temperature. The heat treatment was repeated at least twice and high purity 1:2:4 phases were obtained.

The crystallographic phase identification of the samples was done with an X-ray diffractometer using Cu-K_α radiation. The lattice parameters were determined indexing the (0014), (020) and (200) peaks of the X-ray spectra and also by a Rietveld refinement of the same spectra. It is worth mentioning that the lattice parameters calculated by both

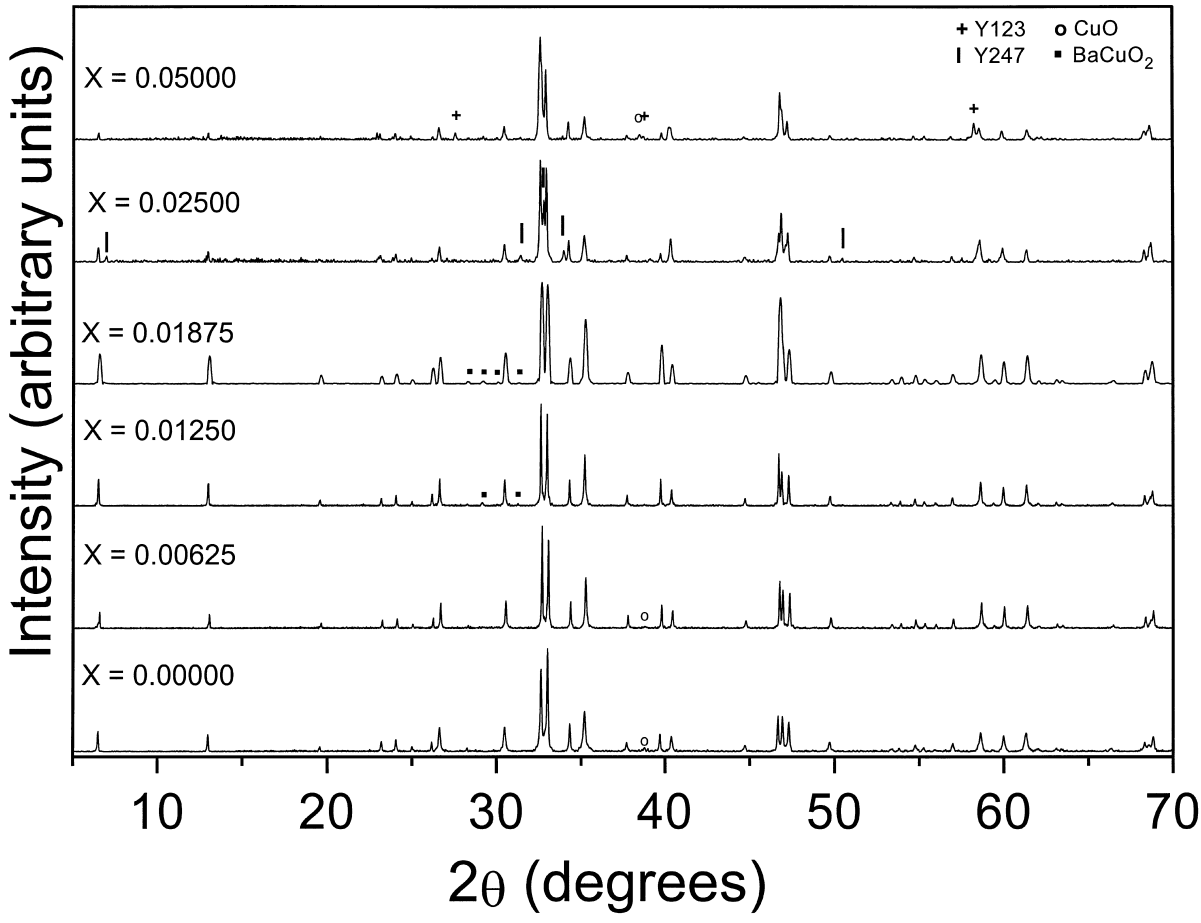

Fig. 2. X-ray diffractograms of the five samples.

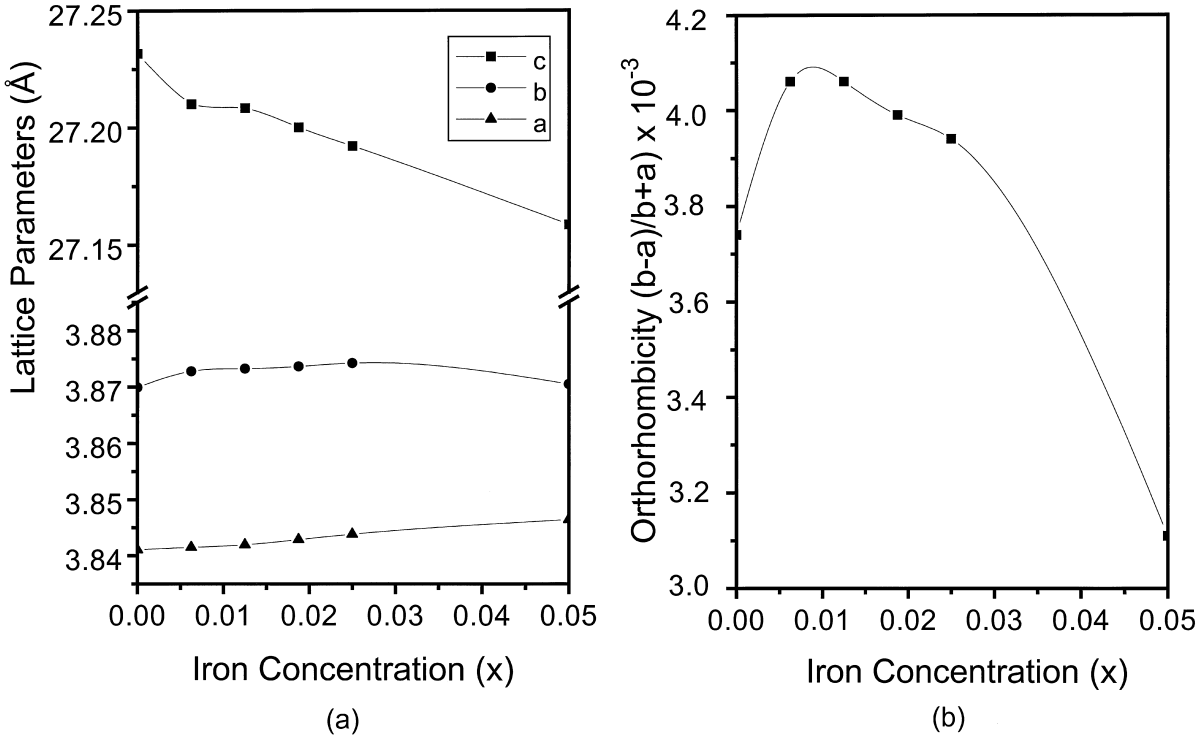

Fig. 3. (a) Crystal lattice parameters and (b) orthorhombicity as a function of iron concentration x.

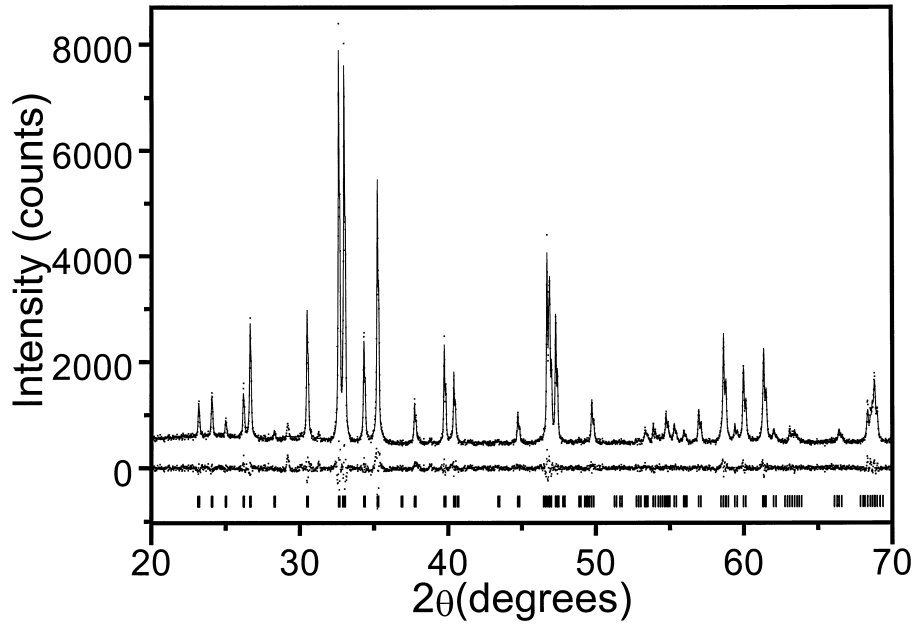

Fig. 4. Rietveld refinement on the X-ray diffraction pattern for the $x = 0.0125$ sample. Experimental spectrum (dots), calculated pattern (continuous line), their difference (middle pattern) and the calculated peak positions (bottom).

procedures are essentially the same. The superconducting transition temperatures were determined measuring the resistance vs. temperature curves, by the standard four probe technique, in a closed cycle helium refrigerator. Room temperature Mössbauer spectra were recorded in transmission geometry with a constant acceleration spectrometer, using a ^{57}Co in Rh source. The spectra were fitted with a constrained least squares program.

3. Results

Fig. 1a shows the normalized resistance as a function of temperature of our samples. As expected, T_c decreases with increasing iron concentration and superconductivity is suppressed for $x > 0.03$. Fig. 1b shows the rate at which T_c diminishes with increasing iron doping; this rate is faster than in the 1:2:3 phase [16,17]. The temperature for zero resistance of the sample with $x = 0.0250$ (in Fig. 1a) is an extrapolated value, and it is indicated as a solid square in Fig. 1b.

Table 1
Rietveld refinement results for the $YBa_2(Cu_{1-x}Fe_x)_4O_{8+\delta}$ structure with $x = 0.0125$

Atom	X	Y	Z	B	N
Cu(1)	0	0	0.2129(1)	1.5(1)	1.936(3)
Fe(1)	0	0	0.2129(1)	1.5(1)	0.048(2)
Cu(2)	0	0	0.0622(2)	2.3(1)	1.984(1)
Ba	1/2	1/2	0.1349(1)	0.89(4)	1.9360(5)
Y	1/2	1/2	0	0.4(1)	0.9560(6)
O(1)	0	0	0.2158(5)	1.5(1)	2.0000
O(2)	1/2	0	0.0515(5)	0.8(5)	2.0000
O(3)	0	1/2	0.0509(5)	0.8(5)	1.760(5)
O(4)	0	1/2	0.1419(5)	0.89(4)	2.0000
O(5)	1/2	0	0.221(2)	1.5(1)	0.536(6)

B (in Å^2) and N are the isotropic thermal and occupancy parameters. The resultant reliability factors were: $R_{wp} = 5.99\%$, $R_B = 3.22\%$, $R_P = 4.76\%$, $R_E = 3.77\%$. The space group is *Ammm* and the calculated crystal parameters (in Å) are: $a = 3.8419(1)$, $b = 3.8730(5)$ and $c = 27.2104(2)$. Numbers in parentheses are estimated standard deviation of the last significant digit.

The main features of the X-ray diffractograms (Fig. 2) correspond to the 1:2:4 structure but, for $x \geq 0.0125$, faint features related to $BaCuO_2$ appear.

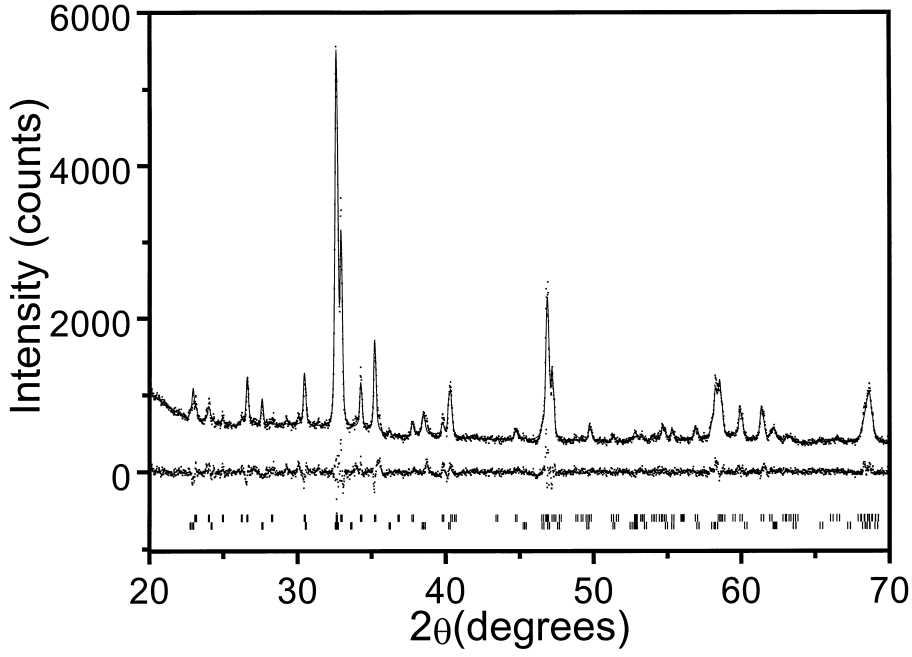

Fig. 5. Rietveld refinement on the X-ray diffraction pattern for the $x = 0.05$ sample. Experimental spectrum (dots), calculated pattern (continuous line), their difference (middle pattern) and the calculated peak positions (bottom). The two series of lines of the calculated peak positions correspond to the 1:2:4 (the one above) and 1:2:3 (the one below) structures.

Table 2
Rietveld refinement results for the $YBa_2(Cu_{1-x}Fe_x)_4O_{8+\delta}$ structure with $x = 0.05$

Atom	X	Y	Z	B	N
Cu(1)	0	0	0.2121(3)	1.3(8)	1.8248(3)
Fe(1)	0	0	0.2121(3)	1.3(8)	0.1128(3)
Cu(2)	0	0	0.0633(2)	1.1(1)	1.928(2)
Ba	1/2	1/2	0.1352(2)	0.55(9)	1.8424(1)
Y	1/2	1/2	0	0.8(3)	0.9584(1)
O(1)	0	0	0.2214(1)	1.3(8)	1.7624(1)
O(2)	1/2	0	0.0634(1)	1.2(7)	2.0000
O(3)	0	1/2	0.0472(2)	1.2(7)	1.7184(1)
O(4)	0	1/2	0.1401(8)	0.55(9)	2.0000
O(5)	1/2	0	0.2147(2)	1.3(8)	0.8736(1)

B (in Å^2) is the isotropic thermal parameter and N the occupancy number. The resultant reliability factors were: $R_{wp} = 6.64\%$, $R_B = 6.41\%$, $R_P = 5.02\%$, and $R_E = 4.05\%$. The space group is *Ammm* and the lattice parameters (in Å) are: $a = 3.8466(1)$, $b = 3.8737(1)$ and $c = 27.1492(9)$. Numbers in parentheses are estimated standard deviation of the last significant digit.

For $x = 0.025$ additional peaks corresponding to $Y_2Ba_4Cu_7O_\delta$ (2:4:7) and CuO impurities are also detected. When $x = 0.05$, the relative intensity of the CuO impurity increases, the 2:4:7 phase features disappear, and new peaks corresponding to the 1:2:3 phase are detected.

For $x = 0.0$, the characteristic triplet of the orthorhombic structure appears at $2\theta \approx 47°$. Using these peaks to measure the a, b, c lattice parameters variations as a function of iron concentration x we observe that the b-parameter remains essentially constant, the a-parameter slightly increases and the c-parameter decreases (Fig. 3a). The orthorhombicity $(b-a)/(b+a)$ as a function of x is shown in Fig. 3b, where a tendency to tetragonality can be observed. This last result qualitatively agrees with recent measurements of the lattice parameters [18,19] that also show this tendency; however they find that

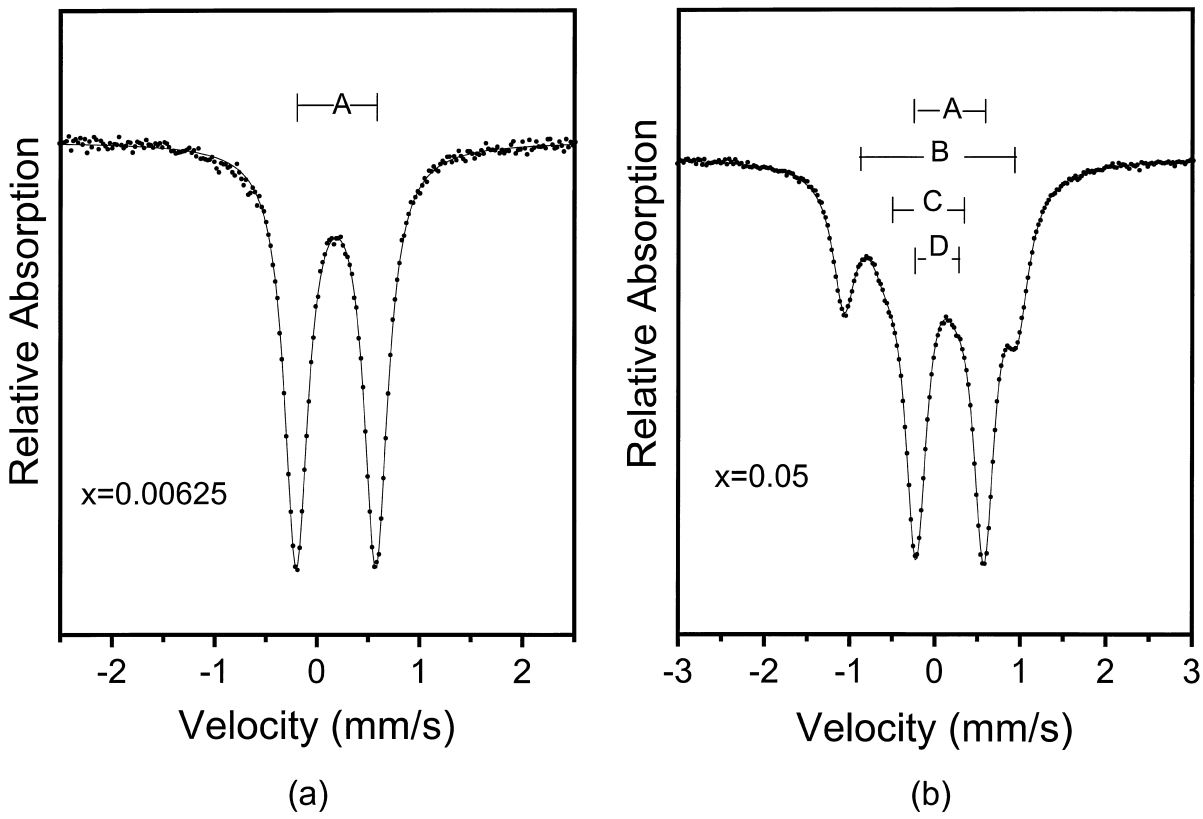

Fig. 6. Mössbauer spectra of the (a) $x = 0.0625$ sample and (b) 0.05 sample.

Table 3
Mössbauer parameters of the five samples

x	IS_A	ΔQ_A	Γ_A	IS_B	ΔQ_B	Γ_B	IS_C	ΔQ_C	Γ_C	IS_D	ΔQ_D	Γ_D
0.00625	0.32	0.78	0.28									
0.0125	0.32	0.78	0.28									
0.01875	0.32	0.79	0.29									
0.025	0.30	0.77	0.26	0.07	1.98	0.35	0.002	0.99	0.31	0.02	0.50	0.31
0.050	0.30	0.79	0.31	0.07	2.02	0.33	−0.06	0.91	0.32	−0.07	0.56	0.27

The isomer shift is with respect to iron and all the figures are in mm/s.

an iron induced orthorhombic to tetragonal transition takes place at around $x = 0.05$.

Rietveld analyses of the samples were done taking into account the different Cu sites where the Fe atoms can go, allowing for the possibility of extra oxygen atoms in two different positions in the structure: O(5), between two adjacent ribbon planes in front of a Cu(1) site, along the *a*-axis, and O(6), between the two adjacent CuO_2 planes above a Cu(2) site, along the *c*-axis. In Fig. 4 we present the $x = 0.0125$ results, as representative of the three low concentration samples, which give place to a single quadrupole doublet in their Mössbauer spectrum (see below). In similar way, Fig. 5 shows the results of the $x = 0.05$ sample, representing the two samples with four quadrupole doublets. In these figures we show the experimental spectra (dots), the calculated patterns (continuous lines), their difference (middle patterns) and the calculated line positions (bars). In $x = 0.05$ sample, the refinement was done considering an admixture of 1:2:4 and 1:2:3 structures, and the two rows of calculated lines shown in Fig. 5 correspond to this assumption. Tables 1 and 2 show the structural parameters, occupation factors, and disagreement factors obtained from these refinements. In these tables, O(1) refers to the oxygen atoms along the ribbons, O(2) and O(3) to the oxygen atoms in the pyramid base along the *a*-axis and *b*-axis, respectively, and O(4) to the oxygen atoms in the Ba atoms plane; O(6) is not included in the tables because its occupation number resulted essentially zero.

Fig. 6a and b show the Mössbauer spectra for $X = 0.00625$ and 0.05, and Table 3 the Mössbauer parameters of the five samples. Each of the spectra for the three lower iron concentrations consist of a single quadrupole doublet, labeled A in Fig. 6a, whose parameters (quadrupole splitting ΔQ, isomer shift IS and line width Γ) remain essentially constant (see Table 3). However, the spectra of the two higher iron concentration samples become more complex and they can only be fitted with four quadrupole doublets, labeled A, B, C and D in Fig. 6b, the most prominent of which (A) corresponds to the single doublet observed at low iron concentrations.

4. ΔQ calculations

The experimental Mössbauer parameters of the quadrupole doublets associated with iron in the Cu(1) sites of 1:2:3 correspond to a high-spin Fe^{3+} state [20] and, consequently, the electron charge distribution has spherical symmetry; hence, there is no contribution of the valence electrons to the electric field gradient (except for polarization effects). This fact suggests that a simple point charge calculation would suffice for an order of magnitude value of ΔQ. It is worth mentioning that even rigorous calculations of the quadrupole splittings when magnetic atoms substitute copper atoms in high-T_c superconductors, normally give values that do not agree with the experimental ones [21,22]. Notwithstanding this fact, ΔQ calculations are normally a good guide to interpret different quadrupole doublets in a complex spectrum. With this in mind, we carried out a simple point charge calculation, in which the (antishielding) Sternheimer factor is taken as a parameter to be fixed by the experimental ΔQ values, for all the possible oxygen environments around the Cu(1) and Cu(2) sites in the 1:2:3 and 1:2:4 structures.

Table 4
Quadrupole splitting calculation for different iron environments

$YBa_2(Cu_{1-x}Fe_x)_3O_\delta$, Fe^{3+} in Cu(1) sites			$YBa_2(Cu_{1-x}Fe_x)_4O_{8+\delta}$, Fe^{3+} in Cu(1) sites		
Coordination	ΔQ	$\Delta Q(1-\gamma_\infty)=6.6$	Coordination	ΔQ	$\Delta Q(1-\gamma_\infty)=6.6$
2	$0.30(1-\gamma_\infty)$	1.980			
3	$0.26(1-\gamma_\infty)$	1.716			
4 planar	$0.29(1-\gamma_\infty)$	1.914	4 planar	$0.28(1-\gamma_\infty)$	1.848
4 non planar	$0.17(1-\gamma_\infty)$	1.122			
5 (pyramidal)	$0.17(1-\gamma_\infty)$	1.122	5 (pyramidal)	$0.14(1-\gamma_\infty)$	0.924
6 (octahedral)	$0.02(1-\gamma_\infty)$	0.132	6 (octahedral)	$0.02(1-\gamma_\infty)$	0.132
Fe(II) or Fe(III) in Cu(2) sites			Fe(II) or Fe(III) in Cu(2) sites		
Coordination	ΔQ	$\Delta Q(1-\gamma'_\infty)=3.2$	Coordination	ΔQ	$\Delta Q(1-\gamma'_\infty)=3.2$
5 (pyramidal)	$0.17\,(1-\gamma'_\infty)$	0.544	5 (pyramidal)	$0.18\,(1-\gamma'_\infty)$	0.576

The components of the electric field gradients are calculated as [23]:

$$V_{ij}=\sum_k Q_k\left(3x_{i,k}x_{j,k}-r_k^2\delta_{ij}\right)r_k^{-5},$$

where q_k are the ionic charges around the site where the electric field gradient is being calculated (the origin), $x_{i,k}$ their rectangular coordinates in the principal axes system, and r_k their distance to the Mössbauer atom (the origin). The magnitude of the quadrupole splittings are calculated as:

$$\Delta Q=\frac{1}{2}qQV_{zz}\left(1+\frac{\eta^3}{3}\right)^2(1-\gamma_\infty),$$

where Q is the quadrupole moment of the nucleus, $\eta=(V_{xx}-V_{yy})/V_{zz}$ is the so called asymmetry parameter and γ_∞ is the Sternheimer factor [24,25]. In Table 4 we show the calculated values of ΔQ around the Cu(1) and Cu(2) sites of both structures. In our calculations we used the value of $Q=0.16$ b, recently determined by Dufek et al. [26] using an ab initio calculation based on linearized-augmented plane-wave band structure method.

5. Discussion

Besides the evolution of the Mössbauer spectra as x increases and the Rietveld analysis results on the crystal structure, three more facts must be taken into account in order to make the site assignment of the iron atoms in the structure: (a) the degradation rate of T_c (b) the tendency to tetragonality and (c) the destabilization of the ribbons into single chains [27,28], all as a function of increasing iron concentration. Because of this last fact, the 1:2:3 Cu(1) sites have to be considered in our analysis. In relation with these three aspects, we present the observations below.

(a) Due to the fact that the charge carriers responsible for superconductivity reside on the CuO_2 planes, the faster degradation rate of T_c with increasing iron concentration suggests Cu(2) site occupancy of the iron atoms. However, as we will see latter, our results indicate that this is not the case.

(b) It is difficult to explain the tendency to tetragonality of the crystal structure if the iron atoms substitute in the Cu(2) sites, because, due to the symmetry of these sites, any possible changes induced by the iron atoms would affect in the same proportion the *a*-axis and *b*-axis dimensions. In fact, all the expected changes, if any, should be along the *c*-axis.

(c) Finally, Yanagizawa et al. [27,28] have shown, by High Resolution Transmission Electron Microscopy (HRTEM), that at around a 3% level of iron doping, a destabilization of the ribbons of 1:2:4 takes place, and that this produces randomly distributed single chains in the 1:2:4 structure.

Our results of the Rietveld refinements for the $x=0.00625$, 0.0125 and 0.01875 samples show that the iron atoms substitute the copper atoms in the Cu(1) sites, in agreement with Felner and Brosh [8] Felner et al. [12]. Moreover the occupation number

for the O(6) oxygen atoms, located in the plane of the Y atoms above the Cu(2) atoms, is essentially zero. The occupation number for the O(5) oxygen atoms, located between the ribbon planes along the *a*-axis, is $N = 0.536$ for $x = 0.0125$ and $N = 0.8736$ for $x = 0.05$. Even though these occupation numbers seem high in relation to the iron concentration, it is possible that the charge redistribution induced by the Fe^{3+} atoms in the ribbon sites allows for extra oxygen atoms in the (large) interstitial space between two adjacent ribbons (see below). The same trend is observed in the $x = 0.05$ sample.

Let us now consider the results of Natali Sora et al. [29] on neutron-diffraction refinement made in the 1:2:3 system when all Cu atoms are substituted by Fe atoms. The authors get a very small occupation number for the above mentioned O(6) atoms (3.5% of the Fe(2) atoms), whereas the occupation number of the O(5) atoms is 2, giving rise to a octahedral coordination of the Fe(1) atoms. Taking into account that all the Cu atoms have been replaced by Fe atoms, their results address the difficulty for oxygen atoms to occupy the O(6) sites, giving support to our interpretation, which differs from those of other authors, that place the Fe atoms mainly (or only) in the Cu(2) site in quasioctahedral symmetry [13,14].

The Mössbauer spectra reported in the literature for the 1:2:3 phase consist of three main quadrupole doublets, which have ΔQs of approximately 2.0 mm/s, 1.10 mm/s and 0.55 mm/s. The only doublet that has been associated with the Cu(2) sites is the one whose ΔQ is around 0.55 mm/s. It is worthwhile mentioning that the combined values of the measured Mössbauer parameters (IS_D and ΔQ_D in Table 3) of this last quadrupole doublet do not permit an unambiguous assignment of the ionic state of the Fe atoms. Actually, they can be in 2 + or 3 + low spin states (in Table 4 we use the notation Fe(II) and Fe(III) for low spin states). From an examination of the calculated values of the ΔQs in Table 4, it can be seen that several of the experimental ΔQ values are reproduced if the Sternheimer factor of Fe^{3+} takes the value $(1 - \gamma_\infty) = 6.6$. Since no two or threefold coordination iron compounds are known, it would be rather unexpected that these coordinations occur in this system, so they should be ruled out from our analysis. It is also clear that the octahedral coordination gives place to ΔQ values which are much to small, so this configuration can also be dismissed. In consequence, the site assignment that we propose is given below.

The 2.0 mm/s doublet is associated with Fe^{3+} in the Cu(1) sites with fourfold (planar) coordination. The 1.10 mm/s doublet is associated with Fe^{3+} also in the Cu(1) sites with fourfold (non planar) coordination and/or with fivefold (pyramidal) coordination. These two possibilities produce slightly different electric field gradients that would broaden the spectral lines. In order to make the site assignment of the 0.5 quadrupole doublet, we recall that Natali Sora et al. results indicate that, at least for the 1:2:3 structure, it is very unlikely that the iron atoms in the Cu(2) sites be surrounded by 6 O atoms in a quasioctahedral coordination. Taking into account this fact, the 0.55 mm/s doublet should be associated with Fe atoms in the Cu(2) sites with fivefold (pyramidal) coordination, despite the fact that our calculations, using the same Sternheimer factor of 6.6, give a quadrupole splitting about half of the observed value. This experimental ΔQ value can be reproduced from the above calculation, using a smaller Sternheimer factor of 3.2. However, it is difficult to explain this low value just in terms of the different ionic state of the Fe atom in the Cu(2) sites. Assuming that the iron atoms are in a Fe(II) state, a possible explanation for the disagreement between the observed and calculated ΔQ values could be that the bonding of the Fe atoms to the apical oxygen atoms has a stronger covalent character (due to the presence of an extra d electron) and this, in turn, could slightly displace them towards these oxygen atoms. Actually, a displacement of 0.03 nm would suffice to get the experimental ΔQ value with the same Sternheimer factor.

Finally, the only compatible situation with the 0.80 mm/s quadrupole doublet value is Fe atoms in the Cu(1) sites in fivefold coordination, notwithstanding the slightly higher ΔQ value obtained in our calculations. In consequence, we suggest that each iron atom at a Cu(1) site attracts an extra oxygen atom that places itself in a vacant site along the *a*-axis between two ribbons. Consequently, the oxygen content of these sites changes. This could explain the observed tendency to tetragonality as the iron concentration increases. The quadrupole doublets B and C observed at the higher Fe doping

levels have the same MP of some of the 1:2:3 doublets, and they can be associated with Fe^{3+} occupying Cu(1) sites of the single chains that result from the destabilization of the double chains. The quadrupole doublet D is associated with Fe(II) or Fe(III) in the Cu(2) sites of the CuO_2 planes.

6. Conclusions

Our Mössbauer results indicate that, albeit that the decreasing rate of T_c with iron concentration is higher for 1:2:4 than for 1:2:3, for low doping levels ($x \leq 0.01875$) the iron atoms occupy only the Cu(1) sites of the 1:2:4 structure. This is in accordance with our X-ray results and also with the HRTEM results of Yanagizawa. At higher doping levels, the ribbon destabilization manifests itself in the X-ray diffractograms, first by the appearance of 2:4:7 and then of 1:2:3 peaks. Similarly, the Mössbauer spectra change from one to four quadrupole doublets, with the new ones corresponding to sites previously identified with the Cu–O single chain sites and with the Cu(2) pyramidal sites. Our calculations and the Rietveld refinement, indicate that, even at low doping level, the iron atoms in the Cu(1) sites attract extra oxygen atoms that place themselves between two adjacent ribbons along the *a*-axis of the structure. If this is the case, the charge distribution around the ribbons will be altered and this, in turn, affects the charge transfer to the CuO_2 planes, with a concomitant effect on T_c. On the other hand, the presence of extra oxygen atoms can have a randomizing effect on the growing directions along the *a*-axis or *b*-axis, that would explain the observed tendency to tetragonality.

In conclusion, our results point in the direction that the excess oxygen between the ribbons explains not only the reported overall tendency to tetragonality of the crystal structure, but also influences the charge transfer mechanism to the superconducting planes and may be the cause of the rapid T_c degradation.

Acknowledgements

The authors acknowledge the help of M.A. Leyva for technical assistance in the Rietveld analysis, to C. Campos-Lozano for assistance in sample preparation and characterization and to C. Munive for helping in the manuscript preparation. This work was supported by DGAPA, UNAM (México), projects IN102095 and IN102896.

References

[1] H. Zandbergen, R. Gronsky, K. Wang, G. Thomas, Nature 331 (1988) 596.
[2] A.F. Marshall, R.W. Barton, K. Char, A. Kapitulnik, B. Oh, R.H. Harnmond, S.S. Laderman, Phys. Rev. B 37 (1988) 9353.
[3] J. Karpinski, E. Kaldis, E. Jilek, S. Rusiecki, B. Bucher, Nature 336 (1988) 660.
[4] D.E. Morris, J.H. Nickel, J.Y.T. Wei, N.G. Asmar, J.S. Scott, U.M. Scheven, C.T. Hultgren, A.G. Markelz, J.E. Post, P.J. Heaney, D.R. Veblen, R.M. Hazen, Phys. Rev. B 39 (1989) 7347.
[5] S. Adachi, T. Sugano, A. Fukuoka, N. Seiji, M. Itoh, P. Laffez, H. Yamauchi, Physica C 233 (1994) 149, and references therein.
[6] P. Marsh, R.M. Fleming, M.L. Mandich, A.M. De Santolo, J. Kwo, Nature 334 (1988) 141.
[7] B.D. Dunlap, J.D. Jorgensen, C. Segre, A.E. Dwight, J.L. Matykiewicz, H. Lee, W. Peng, C.W. Kimball, Physica C 158 (1989) 397.
[8] I. Felner, B. Brosh, Phys. Rev. B 43 (1991) 10364.
[9] R. Lal, S.P. Pandey, A.V. Narlikar, E. Gmelin, Phys. Rev. B 49 (1994) 6382.
[10] M.G. Smith, R.D. Taylor, J.D. Thompson, Physica C 208 (1993) 91.
[11] J.P. Carbotte, M. Greeson, A. Perez-Gonzalez, Phys. Rev. Lett. 66 (1991) 1789.
[12] I. Felner, I. Novik, B. Brosh, D. Hechel, E.R. Bauminger, Phys. Rev. B 43 (1991) 8737.
[13] P. Boolchand, S. Pradhan, Y. Wu, M. Abdelgadir, W. Huff, D. Farrell, R. Coussement, D. McDaniel, Phys. Rev. B 45 (1992) 921.
[14] H.J. Bornemann, D.E. Morris, M.A. Chuev, V.M. Chelepanov, Physica C 199 (1992) 130.
[15] M. Schneider, WYRIET, Version 3, Germany, 1992.
[16] Y. Maeno, M. Kato, Y. Aoki, T. Fujita, Jpn. J. Appl. Phys. 26 (1987) L1982.
[17] J.M. Tarascon, P. Barboux, P.F. Miceli, L.H. Greene, G.W. Hull, M. Eibschultz, S.A. Sunshine, Phys. Rev. B 37 (1988) 7458.
[18] R. Lal, V.P.S. Awana, S.P. Pandey, V.S. Yadav, D. Varandani, V. Narlikar, A. Chhikara, E. Gmelin, Phys. Rev. B 51 (1995) 539.
[19] M. Verma, V.S. Tomar, Solid State Commun. 94 (1995) 925.
[20] R. Gómez, S. Aburto, V. Marquina, M.L. Marquina, C. Quintanar, M. Jiménez, R.A. Barrio, R. Escudero, D. Ríos-Jara, T. Akachi, Mod. Phys. Lett. B 3 (1989) 1127.

[21] A. Saúl, A.M. Llois, A. Levy Yeyati, M. Weissmann, Solid State Commun. 66 (1988) 491.
[22] C. Ambrosch-Draxl, P. Blaha, K. Schwarz, J. Phys.: Condens. Matter 1 (1989) 4491.
[23] N.N. Greenwood, T.C Gibb, Mösbauer Spectroscopy, Chapman & Hall, London, 1971.
[24] R.M. Sternheimer, Phys. Rev. 84 (1951) 244.
[25] R.M. Sternheimer, Phys. Rev. 132 (1963) 1637.
[26] P. Dufek P, P. Blaha, K. Schwarz, Phys. Rev. Lett. 75 (1995) 3545.
[27] K. Yanagisawa, Y. Matsui, Y. Kodama, Y. Yamada, T. Matsumoto, Physica C 183 (1991) 197.
[28] K. Yanagisawa, Y. Matsui, Y. Kodama, Y. Yamada, T. Matsumoto, Physica C 191 (1992) 32.
[29] I. Natali Sora, Q. Huang, J.W. Lynn, N. Rosov, P. Karen, A. Kjekshus, V.L. Karen, A.D. Mighell, A. Santoro, Phys. Rev. B 49 (1994) 3465.